

**EVALUATION OF AN ULTRASONIC TECHNIQUE FOR DETECTING
DELAMINATION IN ASPHALT PAVEMENTS**

Kyle Hoegh
(Corresponding Author)
Research Assistant
Department of Civil Engineering
University of Minnesota
Minneapolis, MN 55455
Phone: 507-398-2669
Fax: 612-626-7750
Email: hoeg0021@umn.edu

Lev Khazanovich, Ph.D.
Associate Professor
Department of Civil Engineering
University of Minnesota
Minneapolis, MN 55455
Phone: 612-624-4764
Fax: 612-626-7750
Email: khaza001@umn.edu

Kenneth Maser
President
Infrasense, Inc.
14 Kensington Road
Arlington, MA 02476
Phone: 781-648-0440
Fax: 781-648-1778
email: kmaser@infrasense.com

Nam Tran, Ph.D.
Research Assistant Professor
National Center for Asphalt Technology
277 Technology Parkway
Auburn, AL 36830
Phone: 334-844-7322
Fax: 334-844-6248
Email: nht0002@auburn.edu

Paper submitted 1 August 2011 in consideration for
Transportation Research Board 91st Annual Meeting,
22-26 January 2012
Words: 4732
Figures: 10
Tables: 0
Photographs: 0
Total Word Count: 7125

**EVALUATION OF AN ULTRASONIC TECHNIQUE FOR DETECTING
DELAMINATION IN ASPHALT PAVEMENTS**

ABSTRACT

Delamination due to layer debonding or stripping between hot mix asphalt layers can cause distresses such as longitudinal cracking in the wheel path and tearing in the surface. Since these distresses cannot be detected by visual inspection of the pavement, Highway Agencies are interested in finding nondestructive methods for detecting delamination to maintain roadway networks. An evaluation of an ultrasonic tomography device in detecting the type and severity of delamination using various focusing techniques is presented in this study. A comparison of blind ultrasonic tomography testing results versus construction of bonded and debonded conditions showed ultrasonic tomography to be capable of detecting delamination between new and old asphalt layers as well as delamination of lifts within new asphalt pavement. Synthetic Aperture Focusing Technique B- and D-scan methods were able to identify delamination between new and old asphalt interfaces while a new focusing method developed at the University of Minnesota was used to identify the delamination within asphalt lifts.

INTRODUCTION

Several types of pavement surface distress can be attributed to delamination between hot mix asphalt (HMA) layers. Longitudinal cracking in the wheel path and tearing in the surface are common types of distress that are caused by delamination between layers. HMA delamination is primarily due to layer debonding or stripping. Debonding occurs when there is inadequate tack between paved HMA layers or due to dirt or other materials. Stripping develops when the aggregates and asphalt binder are incompatible and water separates the asphalt binder from the aggregate. These conditions that cause distress cannot be detected by visual inspection of the pavement. The distress, cracking or tearing, are the first indicators that delamination may be occurring within the pavement layers.

Highway Agencies maintain their roadway network and need a test method to detect the location and severity of delamination before the pavement deficiency causes visual pavement distress. Coring is often used to measure the depth, type, and severity of delamination after the visual distress appears. The objective of this study was to evaluate the effectiveness of a multi-channel ultrasonic technique for delamination detection.

Ultrasonic testing uses high frequency (greater than 20,000 Hz) sound waves that have the capability of detecting defects such as delamination in asphalt. Sound waves are generated by transducers, travel through the material, and are received at the surface. Analysis of the signals by the receiving transducers provides information about the media through which the signal has propagated.

Impact echo testing has been successfully used on concrete structures for applications such as determining thickness, identifying planar flaws such as delamination, and measuring modulus variations (if thickness is uniform). However, impact-echo has experienced difficulties due to the low modulus of asphalt concrete (AC). Spectral analysis of surface waves (SASW) has been more effective with asphalt pavements and has been successfully used for estimating shear modulus and identifying discontinuities in the pavement layers (Schubert and Köhler, 2001; Carino, 2001; Nazarian et. al, 1983).

In this study, dry point contact (DPC) transducers used in ultrasonic tomography have been developed with the capability of transmitting of relatively low frequency (55 khz) elastic waves that penetrate greater depths (Nesvijski, 1997; Mayer et al., 2008). Use of these transducers has been advanced and successfully applied for years in dealing with detailed evaluation of civil structures in Germany (Schubert and Köhler, 2001; Mayer et al., 2008; Khazanovich et al. 2005; Langenberg, K.J. et al., 2001; Marklein, R. et al. 2002). These developments led to MIRA, the state-of-the-art ultrasonic tomography device for diagnostics of civil structures, which utilizes the same principles that have been successful in medical and metal applications (Hoegh et al., 2011).

MIRA utilizes 45 transmitting and receiving channel pair measurements (see figure 1) with 4 transducers in each channel, resulting in an approximately 1 second scan. This gives a 2D depth profile (B-scan) of the subsurface condition directly under the

measurement location. The dry point contact transducers provide the necessary consistency of impact and wavefront penetration to allow for evaluation of heterogeneous mediums such as asphalt. Figure 1 shows a manual MIRA measurement on the left in which the transducers are placed flush to the surface for a B-scan measurement. A B-scan gives 2 dimensional intensity of reflection information indicating changes in acoustic impedance below the scan location. On the right side of Figure 1 the increased redundancy of information of MIRA (bottom) over conventional IE (top) can be observed, where the multi-static array of transmitting and receiving transducers creates 45 measurement angle pairs compared to one measurement pair in traditional IE.

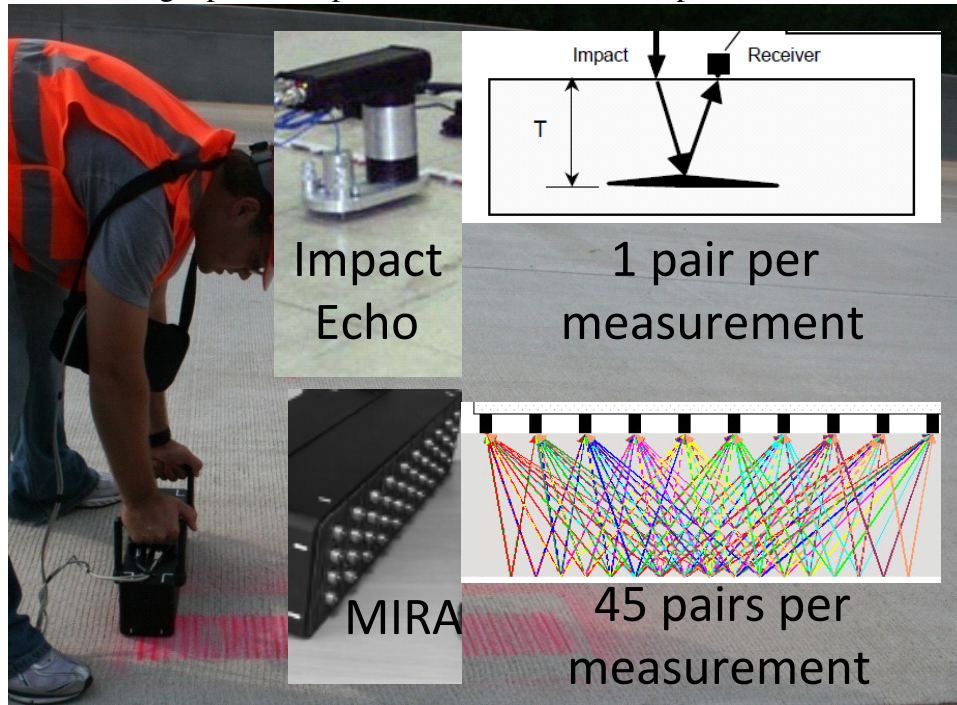


Figure 1. MIRA ultrasonic pitch-catch device and comparison with traditional impact echo method (Carino, 2001).

MEASUREMENT PROCESS AND SIGNAL INTERPRETATION

The left side of Figure 1 shows a MIRA measurement in which the transducers are placed flush to the surface giving 45 different transmitting and receiving measurement pairs. Because the distance between the transducer measurement pairs is constant, the approximate shear wave velocity of the material can be estimated. Since each of the 45 transmitting and receiving pairs within a MIRA scan contain intensity of reflection versus time information, the estimated velocity can be used to reconstruct high intensity locations below each measurement location. One reconstruction method is the Synthetic Aperture Focusing Technique (SAFT) B-scan. SAFT has been found to be a feasible algorithm for use with the ultrasonic pitch-catch technology as well as other applications (Langenberg 1987; Krause et. al, 1997). The basis of the SAFT reconstruction procedure involves (Langenberg 2001 et al.; Marklein, 2002; Hoegh et al 2011):

- 1) Assign the “measured” intensity at every depth in the A-scan from each measurement to all locations in the 180 degree an around the point source
- 2) Apply step 1 for all point sources on the measurement surface
- 3) Use a superposition of the intensity of each A-scan that results in intersection points from the different measurement locations.
- 4) Focus the scatterers by considering these intersections to be the locations of the anomalies.

A SAFT B-scan is a 2 dimensional reconstruction of reflecting interfaces in the concrete directly below the array of transducers with high intensity areas indicating strong reflections due to changes in acoustic impedance. While this is a color-mapped cross-section, it should be noted that each pixel location is associated with the a physical location (depth and lateral position below the array of transducers) and each applied color shade is a result of a combination of intensity of reflection values calculated by the SAFT algorithm based on the location of the sending and receiving transducers, measured velocity, and time after transmission. It should also be noted that in the SAFT B-scan the absolute value of the reflection intensity is taken and the envelope of these values are used in the reconstruction.

Figure 2 shows an example SAFT B-scan taken on a 5-inch thick layer of new asphalt placed over an older asphalt layer. In each SAFT B-scan, the horizontal axis represents the location (in.) along the aperture of MIRA with 0 at the center of the transducer array and the vertical axis indicating the depth (in.) below where the scan was taken. Within B-scans, any change in acoustic impedance (i.e., from AC to air in delaminated asphalt) results in a high intensity image (red/yellow), while areas of through transmission (i.e. sound asphalt) are indicated by a low intensity image (blue) [Hoegh et al. 2010]. It can be observed from Figure 2 that there is a higher intensity area (yellow) where there is an interface between the new and old asphalt layers, indicating debonding between the layers. It can also be observed that there are some moderate intensity (green) areas at shallower depths. Due to the heterogeneous nature of asphalt concrete, there is a baseline amount of scattering and wave attenuation causing a moderate level of intensity that was observed consistently in the various scanned locations regardless of bond

condition. When using SAFT B-scans to evaluate the delamination conditions, only intensities significantly larger than the baseline amount observed due to typical structural noise were considered to be indicative of delamination or stripping.

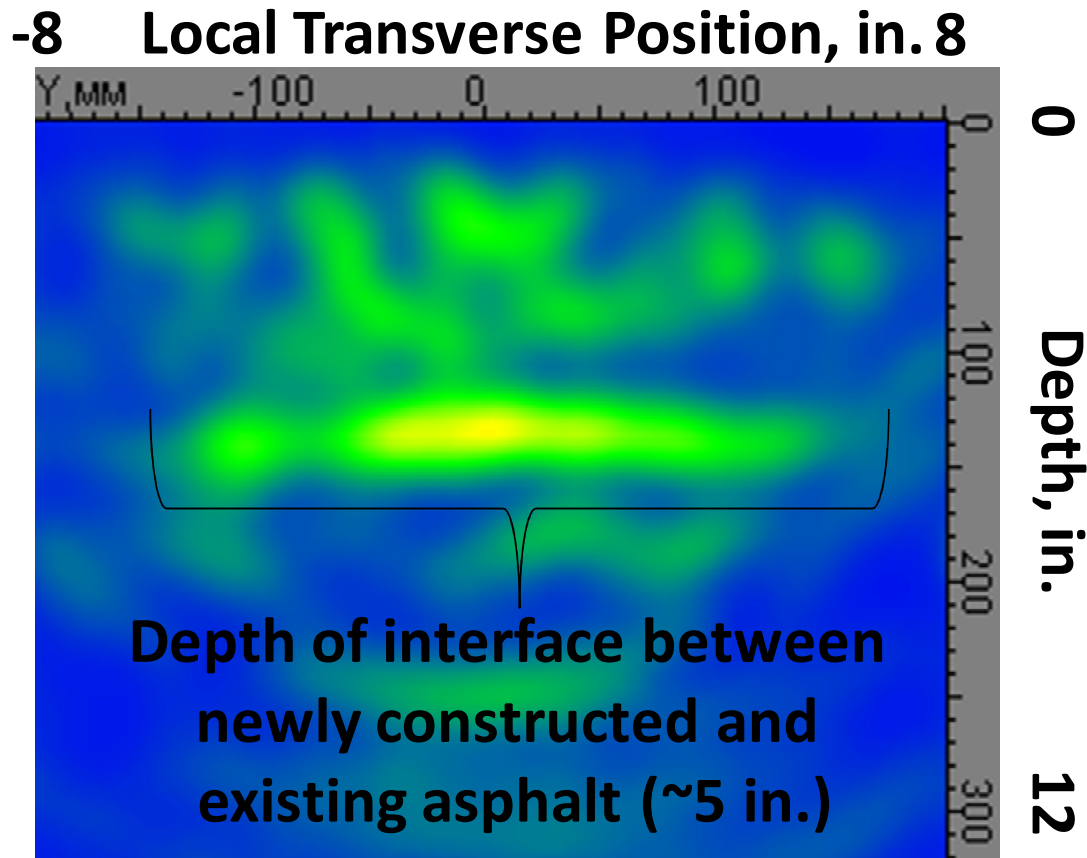


Figure 2. Example SAFT B-scan showing a high intensity of reflection at the depth of the interface between the newly constructed and existing asphalt indicating debonding.

This SAFT B-scan time-of-flight analysis is a powerful tool that can assist in evaluating many applications including delamination at greater depths and more complex geometries where non-planar flaws may be present (Hoegh et al 2011). However, it should be noted that each SAFT B-scan intensity values are normalized relative to the other intensity values within each specific scan. This can cause high intensity reflections within the first 2 inches that do not correspond to shallow delamination in cases where there is a low modulus material such as asphalt. This is caused by unfiltered near field reflections and surface wave arrivals. When delamination at the depth of the asphalt thickness is present, these unfiltered reflections are not as prevalent on the B-scan even though the magnitude of these reflections are similar due to the higher intensity reflection areas at the depth of the delamination. These near field effects are also less prevalent in high modulus material where wave throughout the medium can achieve greater depths. Therefore detecting flaws in the near field at shallow depths (<2 in.) is difficult using SAFT B-scans in material such as asphalt binder. The SAFT Full Waveform (SAFT-FW) B-scan developed at the University of Minnesota uses the basic SAFT

reconstruction procedure, but also accounts for the polarity of the reflected wave by taking account of the whole reflected waveform, rather than the normalized envelope of the absolute intensity of reflection intensity. This analysis proved to be more useful in evaluating these types of shallow planar flaws in this study.

EXPERIMENTAL DESIGN

Construction of Defects

Ten controlled asphalt pavement test sections, built in the inside lane at the NCAT Pavement Test Track, were made available for the controlled field evaluations. These sections had been constructed as part of a SHRP(2) study to investigate a number of NDE techniques for delamination detection. In these sections, conditions of no bond and good bond (control) at the interfaces between dense-graded asphalt layers were created. The construction process ensured the good bond by using a tack coat and bad bond by using bond breakers, including baghouse fines and two layers of heavy kraft paper. Also, a 1-inch thick uncompacted coarse-fractionated RAP material was used to simulate a stripping condition. The scanned sections were not exposed to mechanical loading other than to construction equipment during construction of the outside lane for 2 months in 2008.

The design for the controlled field test sections is illustrated in Figure 3. The test sections were designed to simulate ten different bonded and debonded conditions that represent a majority of situations encountered in the top five inches of HMA pavements. Both full lane width and partial lane debonding conditions were constructed for evaluating various NDT methods. The partial lane debonding condition included wheel path and two 3-ft by 3-ft squared areas. Each test section is 12 ft wide (full paving width) and 25 ft long. To achieve compaction, the full lane width debonded areas were only 10 ft wide. The outer 1-ft was fully bonded to confine the experimental debonded areas for compaction. The detailed design of a typical section (Section 4) is shown in Figure 4. The scope of this paper includes only the 8 sections with an HMA base (Sections 3 through 10).

	Section 1	Section 2	Section 3	Section 4	Section 5	Section 6	Section 7	Section 8	Section 9	Section 10
Top 2-inch lift	Full bond	Full bond	Full bond	Partial No bond	No bond	partial stripping	Full bond	Full bond	Full bond	Full bond
Bottom 3-inch lift	no bond	Full bond	Full bond	Full bond	Full bond	Full bond	Full bond	partial Stripping	partial No bond	No bond
Existing surface	PCC	PCC	HMA	HMA	HMA	HMA	HMA	HMA	HMA	HMA
Section 1 – no bond between 5-inch HMA overlay and PCC pavement Section 2 – full bond between 5-inch HMA overlay and PCC pavement (control section) Section 3 – full bond between 5-inch HMA overlay and HMA pavement (control section 1 of 2) Section 4 – partial bond between 2-inch HMA overlay surface lift and 3-inch HMA overlay leveling lift										

Section 5 – no bond between 2-inch HMA overlay surface lift and 3-inch HMA overlay leveling lift
 Section 6 – simulated stripping in the wheel path between 2-inch HMA surface lift and 3-inch HMA leveling lift
 Section 7 – full bond between 5-inch HMA overlay and HMA pavement (control section 2 of 2)
 Section 8 – simulated stripping in the wheel path between 3-inch HMA overlay leveling lift and HMA pavement
 Section 9 – partial bond between 3-inch HMA overlay leveling lift and HMA pavement
 Section 10 – no bond between 3-inch HMA overlay leveling lift and HMA pavement

Figure 3. Layout of Controlled Field Test Sections.

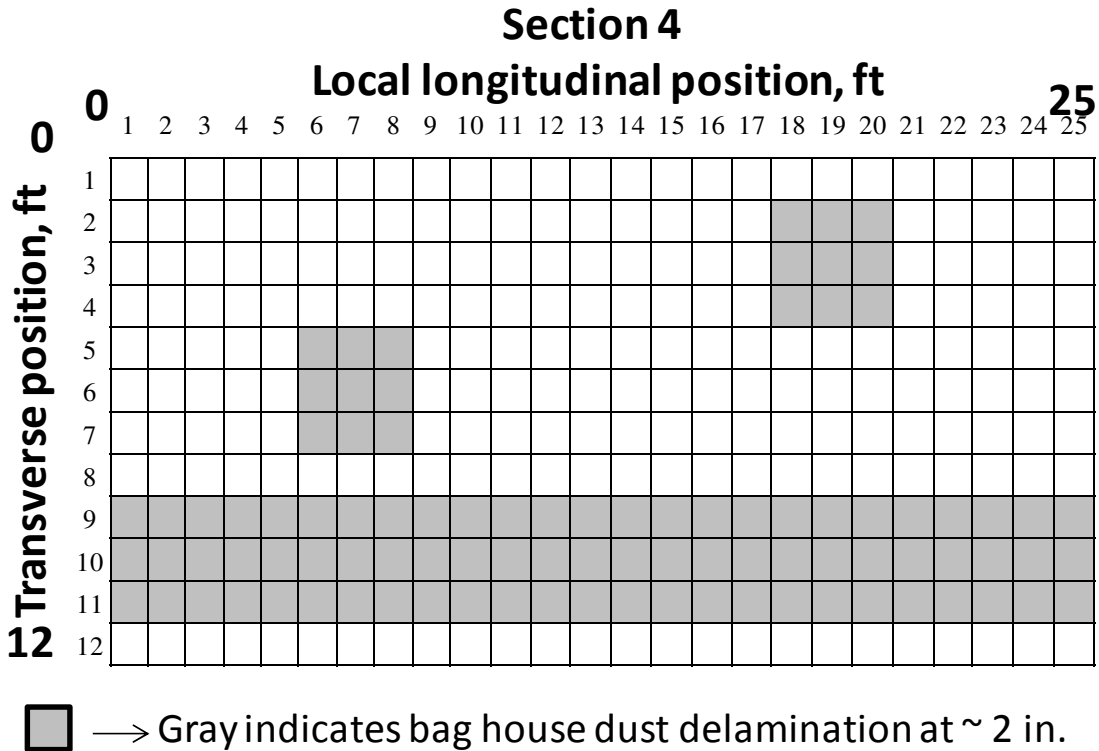


Figure 4. Typical Section: HMA Pavement, Wheel Path Delamination (Station 90 ft through 115 ft.).

MIRA Testing Procedure

The MIRA device was used to conduct a “blind test” of locations with various levels of fabricated distresses at the NCAT Pavement Test Track (NPTT) in Auburn, AL (see Figure 5).

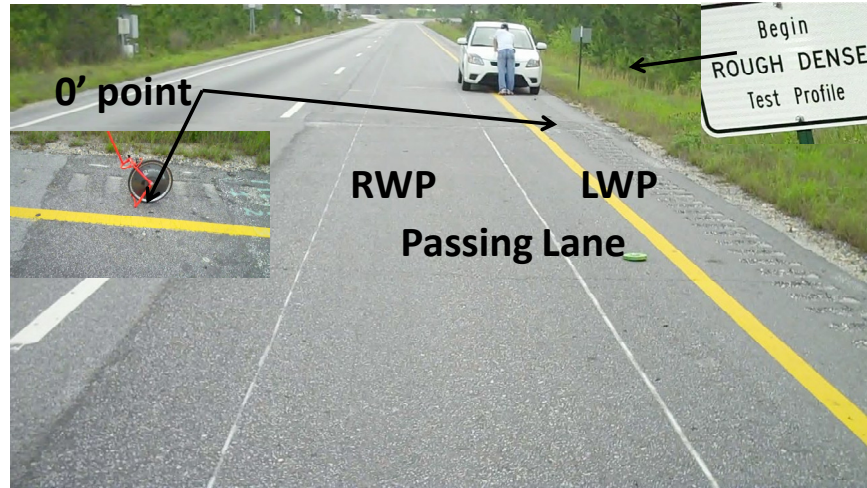


Figure 5. NPTT test site.

NCAT personnel identified the general area where testing was needed to verify the capabilities of MIRA in delamination diagnostics. The tested pavement was separated into eight 25 ft. sections for a total of 200 ft of scanning, with Section 3 starting at 65 ft in the longitudinal direction. MIRA scans were taken with the long portion of the device aperture in transverse and longitudinal orientations at various positions within the 200 ft passing lane section as described below:

- Longitudinal Orientation (see figure 6a)
 - Scan is taken with the long portion of the MIRA device parallel with the direction of traffic. In this orientation, the horizontal axis indicates the longitudinal location with 0 being at the center of the scan location.
- Transverse Orientation (see figure 6b)
 - Scan is taken with the long portion of the MIRA device perpendicular to the direction of traffic. In this orientation, the horizontal axis indicates the transverse location with 0 being at the center of the scan location.

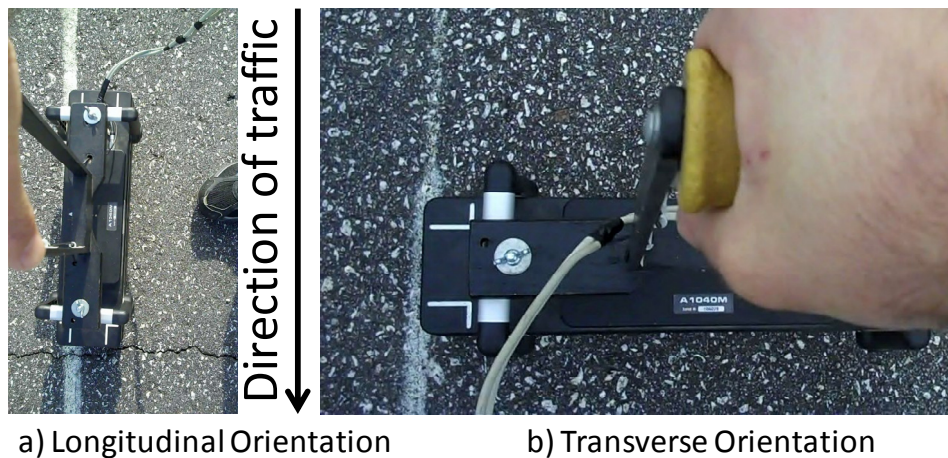


Figure 6. Ultrasonic tomography device (MIRA) in longitudinal (a), and transverse (b) orientations set for transverse and longitudinal step sizes, respectively.

Ultrasonic tomography wave velocity and attenuation is affected by the modulus of the propagation material (Carino, 2001). In addition, asphalt binder modulus is temperature dependant. Thus, since it was important to minimize the effect of temperature variation and sun drenching on the asphalt binder modulus, the testing was conducted starting at 4 AM and ending before sunrise. Although it is preferred to conduct testing at a lower temperature for a higher modulus propagation material and less attenuation, time constraints dictated that the testing was conducted at an approximate temperature of 60 degrees Fahrenheit. Since higher temperatures would likely cause more attenuation, it is recommended that application of the type of testing and analysis presented herein be conducted at 60 Fahrenheit or lower if possible.

Since there was only an approximately 2 hour time window for testing, a full coverage of the 200 ft. by 12 ft. section could not be achieved. As such the testing procedure described below was developed. This resulted in scanning of the full longitudinal length (200 ft.) in both the right and left wheelpaths at approximately 1 ft (~300 mm) step sizes, and scanning of the full transverse length at 1 longitudinal location of each section in approximately 6 in. (~150 mm) step sizes.

Bands of measurements were taken in small step sizes (3 to 6 in.) in the transverse direction with MIRA oriented longitudinally. By stitching these scans together a profile below the surface in the transverse direction along the lane width (D-scan_TV) were realized. This resulted in transverse scans sets with 6 in. spacing at each section for a total of 7 D-scan_TV's. Similarly, bands of measurements taken in the transverse orientation with multiple small step sizes (~1ft) in the longitudinal direction were stitched together to give a profile below the surface in both the right and left wheel paths (D-scan_RWP and D-scan_LWP, respectively). This resulted in longitudinal scans of the right and left wheelpaths at each section at 1 ft spacing for a total of 7 D_scan_RWPs and 7 D_scan_LWPs. These D-scans give a general trend of the amount of reflection occurring at different depths throughout the scanned section by averaging the intensity of reflection across the span of SAFT B-scans used to create the SAFT D-scans.

TESTING RESULTS

SAFT B- and D-Scan analysis was used to detect delamination between new AC and old AC. SAFT-FW B-Scan analysis was used to detect delamination between new AC lifts. The data interpretation approach for these analysis methods is presented including explanation of example scans indicating the following cases:

- Delamination between new and old asphalt
 - SAFT D-scan example: Figure 7 at wheelpath locations
 - SAFT B-scan example: Figure 2.
- No delamination between new and old asphalt
 - SAFT D-scan examples: Figure 7 at non-wheelpath locations and Figure 8
- Delamination between lifts
 - SAFT-FW B-scan example: Figure 10-top

- No delamination between lifts
 - SAFT-FW B-scan example: Figure 10-bottom

Delamination/Stripping at Asphalt/Base Interface

SAFT B- and D-scan analysis allowed for identification of no-bond or stripping conditions at the depth of the newly constructed asphalt. SAFT D-scans could be created when multiple SAFT B-scans were taken in small step sizes (3 in. to 6 in.) and fused together. The vertical axis of the D-scan is the depth below where each B-scan was taken, while the horizontal axis now includes the entire range of testing in the set of B-scans taken. Therefore, instead of analyzing each individual SAFT B-scan, patterns that emerge from the entire right and left wheel paths for SAFT D-scan_RWP or SAFT D-scan_LWP, respectively, or the entire lane width for SAFT D-scan_TV can be analyzed.

The intensity of reflection occurring at different depths throughout the scanned section is determined by averaging the intensity of reflection across the aperture of the device in each individual B-scan. Therefore, SAFT D-scans can be analyzed in a similar manner to the individual SAFT B-scans, while getting a more complete view of trends throughout the section. In this manner high intensity of reflections indicate delaminated areas with the vertical location indicating the depth of the delamination, and the horizontal location indicating the position within the Section where the delamination was occurring. As briefly mentioned in the introduction, there are also high intensity reflections within the first 2 inches in many of the SAFT B- and D-scans. These shallow depth reflections could not be differentiated from lift delamination in the conditions of this study so they were disregarded when using this type of analysis. SAFT-FW B scans were used exclusively for analysis of shallow defects such as lift delamination.

Section 9, where the no-bond condition was only constructed in the wheelpaths, gives a good example of how SAFT D-scan analysis was able to diagnose and pinpoint the delamination between old and new AC. MIRA scans were taken across the transverse direction of Section 9 starting in the left wheelpath and moving towards the centerline allowing for creation of the SAFT D-Scan_TV shown in Figure 7. In this SAFT D-Scan_TV the horizontal axis is approximately 12 ft from the left wheel path toward the joint centerline and the vertical axis is approximately 1 ft in depth below the surface. High intensity of reflection areas are indicated by yellow/red locations. It can be observed from the SAFT D-scan_TV shown in Figure 7 that there are high intensity of reflection areas at the depth and lateral spacing of the left and right wheel paths. This reflection is absent (blue) in the non-wheel path lateral locations at the same depth. Thus, during the blind test analysis it was concluded that there was delamination at the wheel path locations, while the asphalt is fully bonded at the non-wheelpath locations. This was verified by the constructed no-bond condition in the wheel paths of Section 9.

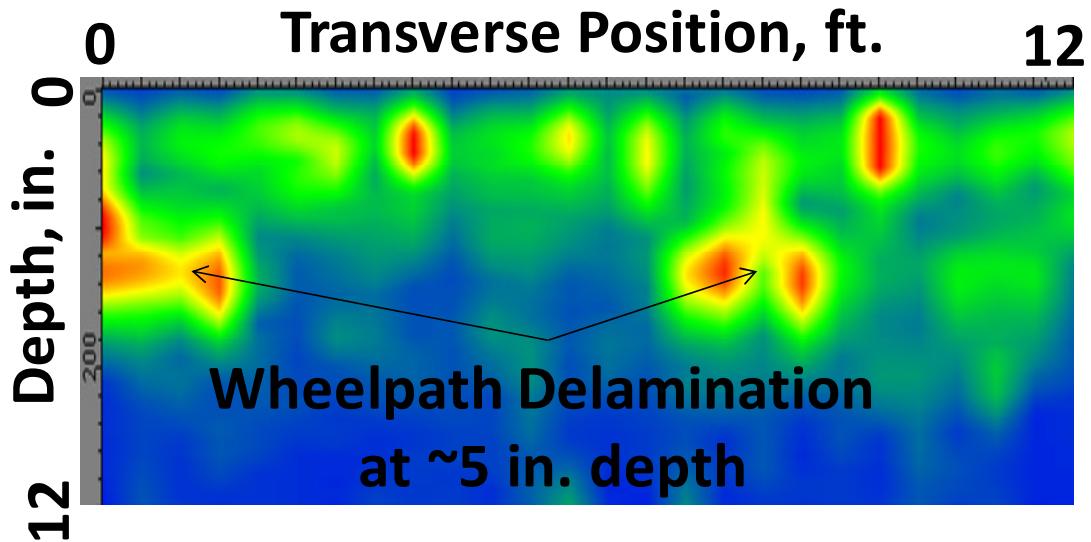


Figure 7. SAFT D-scan_TV indicating delamination between the existing asphalt and newly constructed asphalt in the wheelpath.

Using this type of SAFT D-scan analysis, locations where high intensity of reflection (yellow/red) was observed at the approximate boundary depth between the new and old AC interface indicated delamination, while the absence (blue) of high intensity of reflection at that depth indicated a bonded condition. Figure 8 shows a SAFT D-scan_LWP where a full bond at the depth of the new and old asphalt interface was observed. Figure 7 shows the last 15 ft. of Section 3 and first 10 ft. of Section 4. It can be observed that there is no high intensity of reflection areas at the depth of the newly constructed asphalt in these sections.

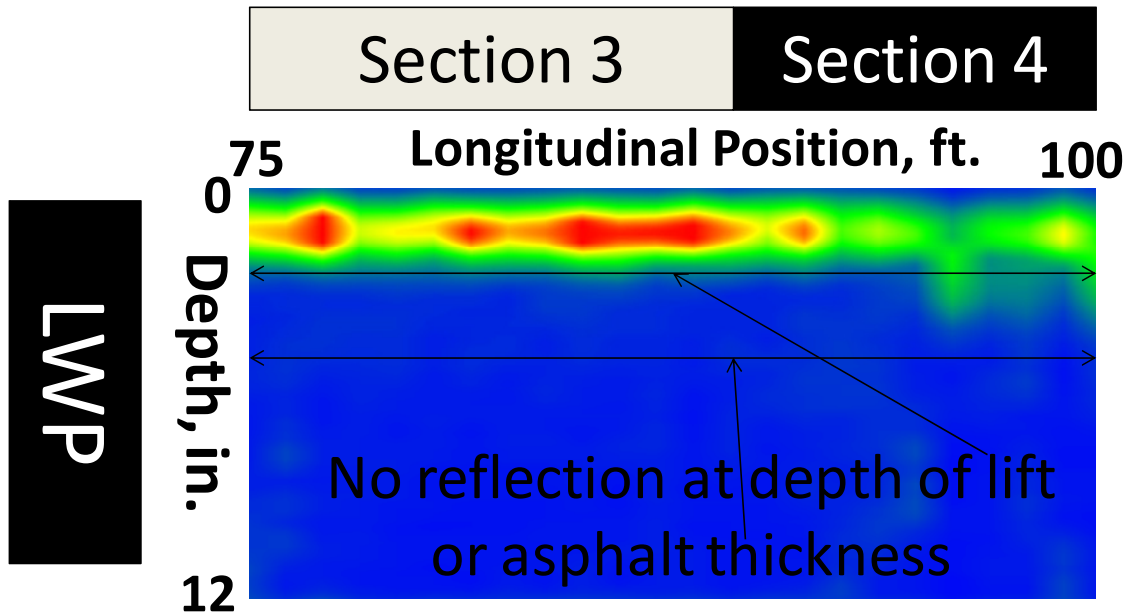


Figure 8. SAFT D-Scan_LWP indicating a full bond between the newly constructed asphalt and HMA base.

This type of blind testing analysis was used to correctly identify bonded or delaminated conditions resulting in detection of delamination at the no bond construction in Section 10, and stripping in the left wheel path of Section 8, as well as the full bond in Sections 3 through 7.

Lift Delamination

Detection of delamination fabricated between asphalt lifts was also diagnosed by MIRA, although a more detailed analysis was required. Since there is a certain level of near field reflections at 2 inches or less in the B or D-scans similar in intensity to delamination at the 2 in. asphalt lifts in this study, it was more difficult to resolve lift delamination using MIRA. The same Figure 8 SAFT D-scan_LWP, used to show a full bond at the base depth in the previous section, can be used to illustrate the difficulties in using SAFT B or D-scans to identify delamination at depths at approximately 2 inches in this study. It can be observed that there is no clear difference in reflection intensity at the change from Section 3 to Section 4 despite the different constructed conditions at the 2 in. lift.

In these cases, SAFT-FW was necessary to detect the presence of delamination. Using SAFT-FW analysis multiple reflections (resonance) in intervals of approximately 2 in. indicated delamination at the 2 in. lift. Since the multiple reflections occurred well after surface wave arrivals, they could be effectively resolved to identify locations where 2 in. lift stripping or delamination occurred.

To illustrate the capabilities of detecting delamination between asphalt lifts using SAFT-FW, Sections 5 and 7 are examined. In section 5, the lift was constructed using baghouse fines and kraft paper, while a full bond was constructed in Section 7. Figure 9 shows an example SAFT B-scan of Section 5 (top) and Section 7 (bottom). The depth of each scan shown is approximately 1 ft. Similar to the SAFT D-scans, there is no clear difference in the SAFT B-scans between the two Sections. At such a shallow depth (2 in.) the initial arrival from the delaminated interface could not be resolved in the SAFT-B-scans. Figure 10 shows the same measurement locations using SAFT-FW analysis. Section 5 is shown on the top and Section 7 on the bottom with approximately 1 ft of depth shown in each scan. While the scans were inconclusive using SAFT B- and D-scans, multiple reflections at shallow intervals (approximately 2 in.) can be seen in the Section 5 SAFT-FW B-scan, while these reverberations are absent in the Section 7 SAFT-FW B-scan. The resonance correctly indicated the presence of no-bond in Section 5 and absence of reverberations indicated a fully bonded lift in Section 7.

Multiple reflections were also observed in a few of the Section 4 scan locations and present to a lesser extent in the Section 6 scan locations. Multiple reflections were not observed in any of the Section 3, 7, 8, 9, or 10 locations. This resulted in the correct blind testing identification of partial stripping in Section 4, no-bond in Section 5, and partial no-bond in Section 6 as well as full bond in the remaining sections.

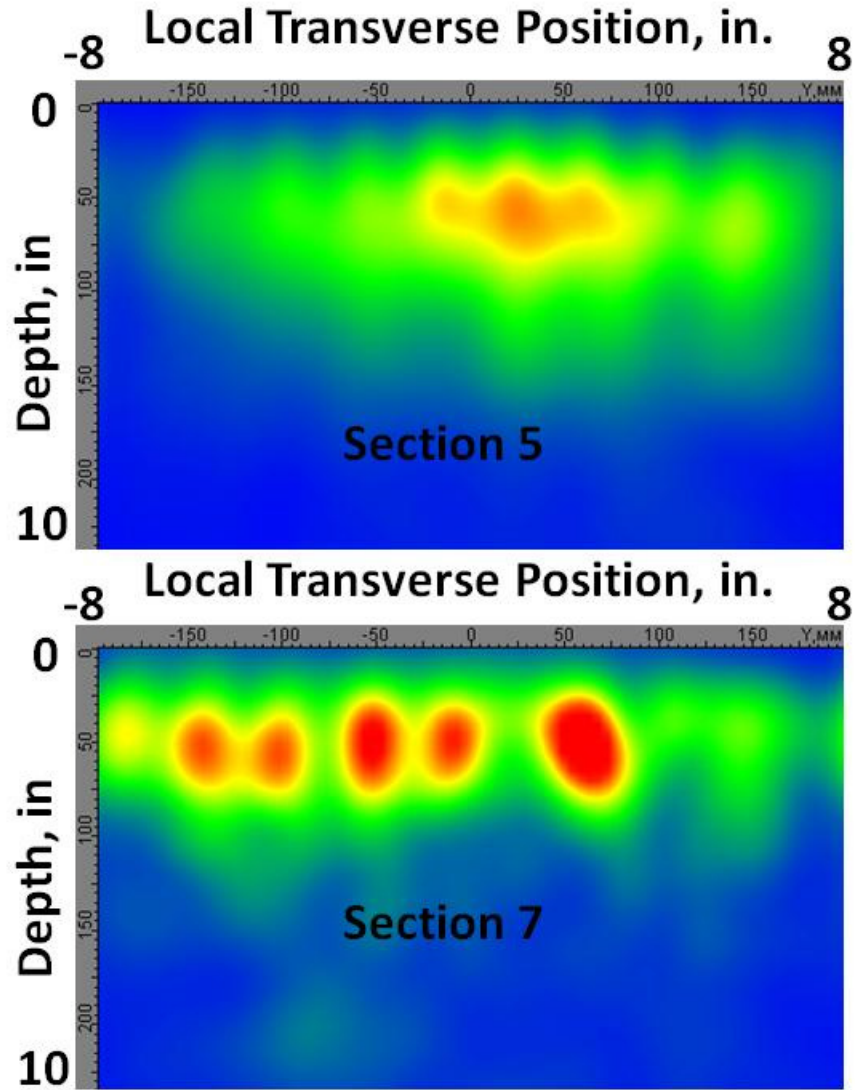


Figure 9. Section 5 (top) and 7 (bottom) example B-scan locations.

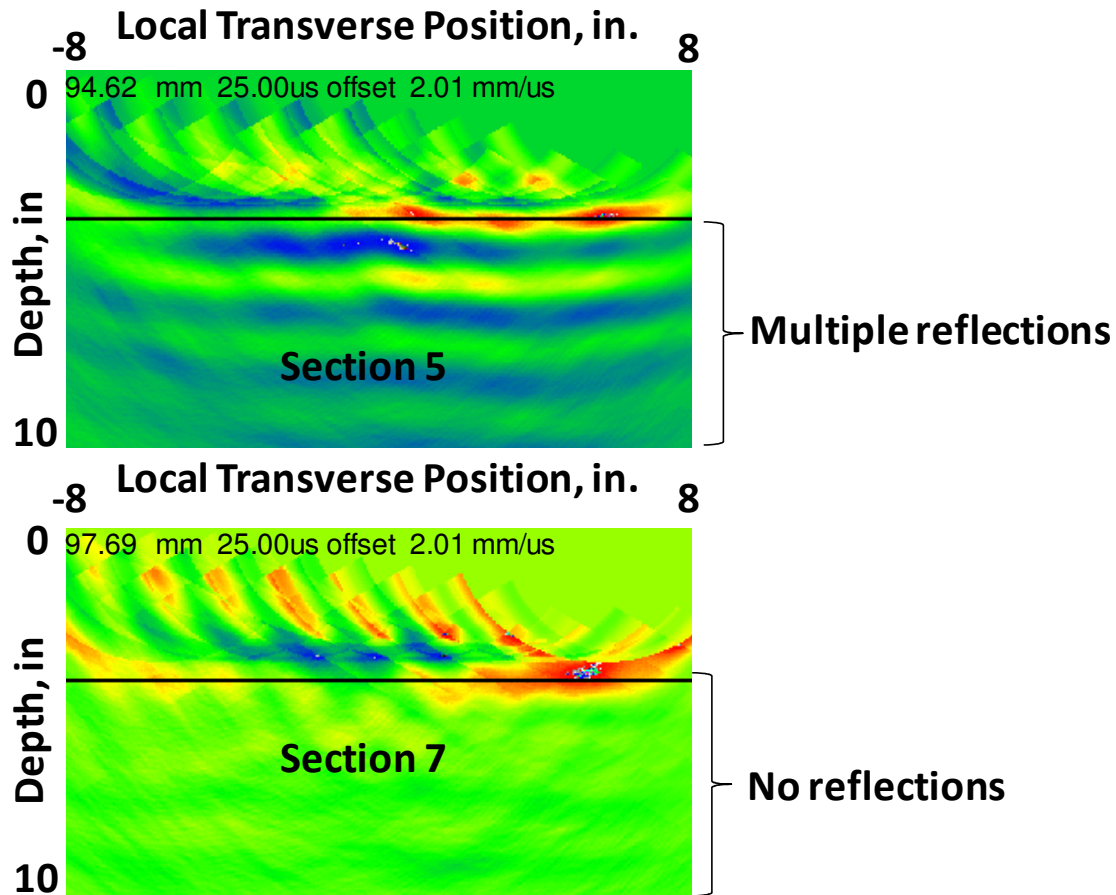


Figure 10. SAFT-FW B-scans showing multiple reflections in the Section 5 location and absence of multiple reflections in the Section 7 location.

It should be noted that while 2 in. depth delamination required SAFT-FW analysis under the conditions of this study, this does not necessarily mean that this is the case for different asphalt or delamination conditions. For instance, higher asphalt binder temperature and subsequent lower binder modulus reduces the wave penetration and thus increases the difficulty in filtering near field reflections from shallow delaminations. More testing should be conducted to identify testing criteria such as a cutoff depth for when SAFT-FW is necessary to identify new lift delamination under different binder temperature conditions.

Blind Testing Results Summary

The following summarizes the diagnoses that were made based on the blind test results for Sections 3 through 10 prior to the construction results being revealed:

- Section 4: Slight level of delamination
- Section 5: Significant level of delamination
- Section 6: Very slight delamination
- Sections 3, 7: Inconclusive using current analysis method.

- Section 8: Delamination between newly constructed asphalt and asphalt base at the beginning (190 ft to 200 ft) of the LWP.
- Sections 9, 10: Newly constructed asphalt debonded with asphalt base in RWP and LWP

It should also be noted that the blind testing results of ultrasonic tomography testing successfully pinpointed the delamination locations in the wheelpath at the interface of new and old AC at the partial no-bond location. SAFT-FW analysis of the partial “no bond” and partial stripping lift sections only allowed for the conclusion that part of the section was delaminated while the wheelpath vs non-wheelpath distinction was not made in time before the construction results were revealed.

CONCLUSIONS

As can be observed from a comparison of the testing results versus the constructed defects, ultrasonic tomography proved to be capable of detecting delamination at the interface between the new and old AC, delamination at 2-in. depth between two new lifts and a slight indication of stripping at the base of a new 2-in. lift. Analysis of “canned” SAFT B and D-scans showed that delamination at approximately 5 in. depths where stripping or no-bond conditions were present. SAFT-FW analysis was required for diagnosis of the 2 in. depth asphalt lift condition. The current SAFT B-scans can be reconstructed into SAFT D-scans to get a more complete picture of the section, while the current SAFT-FW analysis only allows for individual B-scan analysis. This SAFT-FW analysis should be expanded in the future to allow for identification of larger trends. In addition, more testing should be conducted to calibrate the effect of different binder types and temperature conditions on ultrasonic tomography testing. This will allow for establishment of field testing protocol such as identification of what lift depth requires SAFT-FW B-scan analysis rather than the “canned” SAFT B-scan analysis at various environmental conditions. The testing procedure and results suggest that an initial screening with higher speed nondestructive methods might complement the ultrasonic tomography method. In this case the required testing coverage could be reduced by targeting only areas that are suspected to be delaminated for more detailed testing with the method presented in this paper.

ACKNOWLEDGMENTS

The authors would like to thank the Strategic Highway Research Program 2 for sponsoring part of the research presented in this study. The NCAT personnel should also be acknowledged for providing the site and assisting with the testing.

REFERENCES

Carino, N.J., *The Impact-Echo Method: An Overview*, Proceedings of the 2001 Structures Congress & Exposition, May 21-23, 2001, Washington, D.C., American Society of Civil Engineers, Reston, Virginia, Peter C. Chang, Editor, 2001.

Hoegh K., Khazanovich L., Yu H.T. “Ultrasonic Tomography Technique for Evaluation of Concrete Pavements. Transportation Research Board 90th Annual Meeting. Report Number: 11-1644 Pre-print (Accepted for Publication). 2011.

Khazanovich, L., R. Velasquez, and E. Nesvijski (2005). “Evaluation of Top-Down Cracks in Asphalt Pavements Using a Self-Calibrating Ultrasonic Technique” *Transportation Research Record: Journal of the Transportation Research Board*, No. 1940, pp. 63–68.

Krause, M., Muller, W., and Wiggerhauser, H. “Ultrasonic inspection of tendon ducts in concrete slabs using 3D-SAFT.” *Acoust. Imaging*, 23, 433–439. 1997.

Langenberg, K.-J. “Applied inverse problems.” *Basic methods of tomography and inverse problems*, P. C. Sabatier, ed., Adam Hilger, Bristol, England. 1987.

Langenberg, K.J. et al. *Inverse Scattering with Acoustic, Electromagnetic, and Elastic Waves as Applied in Nondestructive Evaluation*. Chapter 2 in *Wavefield Inversion*. Edited by Armand Wirgin (2001).

Marklein, R. et al. *Linear and Nonlinear Inversion Algorithms Applied in Nondestructive Evaluation*. University of Kassel. *Inverse Problems* (2002). Inst. of Physics Publishing.

Mayer, Klaus et al. *Characterization of Reflector Types by Phase-Sensitive Ultrasonic Data Processing and Imaging*. *Journal of Nondestructive Evaluation* (2008). Springer Science. Pp. 35-45.

Nazarian, S., Stokoe II, K.H., Hudson, W.R. *Use of Spectral Analysis of Surface Waves Method for Determination of Moduli and Thicknesses of Pavement Systems*. *Journal Transportation Research Record: Journal of the Transportation Research Board*, Issue # 930, ISSN 0361-1981. pp. 38-45, 1983

Hoegh, Khazanovich, Maser and Tran

Nesvijski, E.G., "On the Problem of Application of the Conic and Exponential Wave Guiding Extensions for Ultrasonic Transducers for Materials Testing". Journal: NASTA Technical Bulletin, Philadelphia, PA, USA, 1997 (ISSN 1079-8498), Volume 3, pp. 49-56.

Schubert, Frank and Köhler, Bernd. *Three-Dimensional Time Domain Modeling of Ultrasonic Wave Propagation*. Fraunhofer Institute for Nondestructive Testing, Dresden Germany. Journal of Computational Acoustics (2001). IMACS. pp. 1543-1560.